Websites:
http://www.sciencepub.net/nature
http://www.sciencepub.net

Emails:
naturesciencej@gmail.com
editor@sciencepub.net

Nature and Science

MARSLAND PRESS
Multidisciplinary Academic Journal Publisher

Attenuation of Gamma Radiation in Different Materials

Ahmed Alharbi

Department of Physics, Qassim University, Qassim 51452, Kingdom of Saudi Arabia
qu.c@hotmail.com

Abstract: Shielding materials for nuclear gamma radiations are of prime importance for radiation protection and safety in applied nuclear radiation fields. In this study, the experimental investigation of attenuation properties by using NaI (TI) scintillator was performed for a lead (Pb) absorbing material with various thickness at the photon energy 661 keV. The obtained result revealed that lead is an effective absorbing material for gamma rays with a high linear attenuation coefficient (μ_{Pb}= 0.111□□$^{-1}$). Furthermore, the experimental data of the linear attenuation coefficient was compared with the XCOM theoretical calculation and a good agreement has been observed. In addition, the sensitivity of both the NaI(TI) detector and the Geiger Muller counter was determined at various distances from a ^{99}Tc source. Therefore, the experimental values showed that the NaI(TI) scintillator is a high sensitive to gamma ray source, whereas an extremely low sensitivity was obtained from the Geiger Muller detector. This concludes that the NaI(TI) detector is an appropriate detector for nuclear medicine applications. These results indicate that the processes performed in this study can be followed by future work in order to calculate the attenuation properties of other absorbing materials at different gamma-ray energies as well as the sensitivity of other type of detectors.
[Ahmed Alharbi**. Attenuation of Gamma Radiation in Different Materials.** *Nat Sci* 2024,22(3):40-47]. ISSN 1545-0740 (print); ISSN 2375-7167(online). http://www.sciencepub.net/nature 04. doi:10.7537/marsnsj220324.04.

Keywords: gamma-rays ; Shielding materials; gamma-rays attenuation

1. Introduction

The study of the interaction of gamma rays with different shielding materials is of great importance in basic physics. This study is also significant for radiation protection purposes in several nuclear radiation fields such as and medical hospitals, storage of radioactive materials, nuclear reactors, and environmental application. Although there are three major approaches for radiation safety namely time, shielding, and distance, radiation shielding is the most commonly used method. This technique depends on the principle of attenuation, which is attributed to the gradual reduction of radiation intensity traversing a thickness of an absorber [1]. Therefore, the appropriate thickness of a shielding material required for radiation protection can be calculated once the radiation attenuation determined. Furthermore, in radiation measurement studies, various detectors such as gaseous detectors, scintillation detectors, and semiconductor detectors can detect g-rays. In such detectors, an inclusive understanding of their spectral performance is paramount to identify the types of radiation and their intensities. Thus, this can lead to selecting the proper detector for a given radiation source[2]. This report aims to determine the gamma ray attenuation properties of a lead absorber by utilizing The NaI(TI) scintillator as well as the absolute sensitivity of both Geiger Muller detector and the NaI(TI) detector.

2. Theory

2.1 Gamma Ray Interaction with Matter

Gamma rays are a high energy and penetrating electromagnetic radiation arising from the atomic nucleus. Such radiations are categorized indirectly ionizing radiations and can be absorbed, scattered or transmitted through the interaction with absorbers and detectors by three major processes: photoelectric effect (photoelectric absorption), Compton scattering, and pair production.

2.1.1 Photoelectric Effect

A gamma ray may interact with a bound atomic electron (an atomic interaction) in such a way loses all of its energy in one interaction. Therefore, an atomic electron called a photoelectron will be released with kinetic energy E_k when the energy of incident gamma photon E_γ is higher than the binding energy of the atomic electron BE .

$$E_k = E_\gamma - BE \qquad (1)$$

The photoelectric effect is paramount because it can form a full-energy peak (photo peak) as a result of a complete absorption of gamma rays in the detector material. The probability for this process is directly proportional to z^4/ E_γ^3 , which means it significantly depends on the atomic number of the absorbing material (Z) and gamma-ray energy(E_γ) .Thus, this concludes that such an interaction is dominant for

heavy elements and low-energy gamma rays (E_γ < 500 keV)[3].

2.1.2 Compton Scattering

Compton scattering is an inelastic collision of a gamma-ray photon and a very loosely bound electron in the absorbing materials and detectors. Thus, the gamma ray photon transfers some of its energy to an atomic electron of the material. The energy of the electron and the deflected gamma ray $E_{\gamma`}$ after scattering depends on the energy of the incident photon E_γ, and the angle of deflection (θ) (Figure1).

$$E_{\gamma`} = \frac{E_\gamma}{1+\frac{E_\gamma}{m_e c^2}(1-cos\theta)} \quad (2)$$

where c is the speed of light and m_e is the electron mass and. The maximum kinetic energy transferred to the electron occurs when the photon is scattered backwards through an angle of 180°. The Compton edge stems from the energy of the scattered electron deposited in the detector material. While the backscatter peak is formed when the gamma ray deflects with a large angle (120º-180º) in the shielding material surrounding the detector before being absorbed in the detector. Compton interaction probability is proportional to $\frac{Z}{A}$ (the atomic number Z per unit mass A) and is nearly constant for all materials.

2.1.3 Pair Production

This process occurs only when the energy of the gamma ray exceeds 1.022 MeV that equals the sum of the rest mass of the electron and the positron. In such an interaction, the incident photon interacts with the Coulomb field of the atomic nucleus, which is then converted into matter in the form of a positron-electron pair according to Einstein's mass and energy equivalence principle.

$E = m_e c^2$ (3)

where E is the energy of the gamma ray and m_e is the rest mass of the electron.

2.1.4 Attenuation of Gamma Rays

When a gamma radiation penetrates an absorber, the intensity of the radiation undergo attenuation primarily by photoelectric effect, Compton scattering, and pair production interactions as a function of the absorbing material thickness according to the Beer's law.

$I=I_0 e^{-\mu x}$ (4)

where I_0 is the intensity of gamma ray with the absence of the absorber, I is the attenuated gamma ray intensity transmitted through an absorber of thickness x, μ (cm^{-1}) is the linear attenuation coefficient of the absorbing material. The half-value thickness of the absorber, which reduces 50% of the incident gamma ray radiation can be determined as follow [4].

$x_{1/2} = ln2/\mu$ (5)

3. Apparatus

The experiment has been achived by utilizing different gamma ray sources (^{22}Na, ^{137}Cs and ^{60}Co), a power supply, lead absorber (pb) ,the NaI(TI) scintillator which is connected to a multi-channel analyzer , and Geiger Muller detector as well as root analysis software.

3.1 NaI(TI) Detector

The (2×2 inch) NaI(Tl) scintillator contains an inorganic material (Sodium Iodide crystal) which is activated by thallium iodide (Tl) coupled to a photomultiplier tube (PMT). In this detector, the incident γ-ray radiation can interact with the electrons in the scintillating crystal (NaI) by three primary mechanisms: photoelectric effect, Compton scattering and pair production. Therefore, these electrons can be released and cause ionization of the NaI crystal, which fluoresces by converting ionization energy to visible photons. The number of scintillation photons depends on the energy of the incident γ-ray and up to 40,000 photons can be produced per 1 MeV gamma photon. These yielded photons are Poisson-distributed random variables and only some of them will eject photoelectrons from the surface of photocathode. Thus, these electrons are then multiplied by dynodes in the PMT (Figure1). The amplified output pulses of the PMT are analyzed and converted to digital signals by an Analog to Digital Converter (ADC).They are then sorted depending on their arrival time and amplitude in the multichannel analyzer [5].

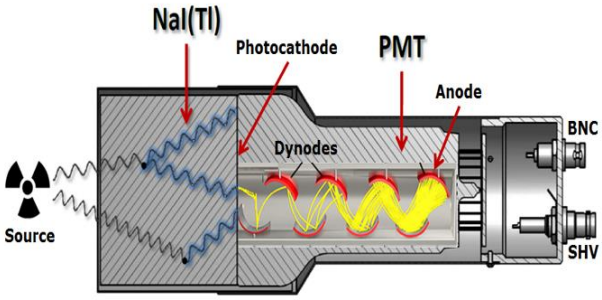

Figure 1. Schematic diagram of the detector with NaI(Tl) crystal and PMT [6].

The NaI(Tl) scintillator is commonly used in nuclear medical imaging which forms an image after measuring the intensity of gamma ray emitted from the patient's organ [2].

3-2 Geiger Muller Detector

Geiger Muller detector (Geiger-Muller tube) is gaseous ionization detector, which consists of a cathode and a central wire anode surrounding by gas. These electrodes have a high voltage across them. When the incident radiation enters the tube, it can ionize the gas. Consequently, the electrons move to the anode and the ions are attracted to the cathode. This will produce an electrical current, which can be measured as counts. is proportional to the incoming radiation energy.

4. Experimental Setup

4-1 Calibration

Calibration of the NaI(Tl) detector is essential before being used in radiation measurements in order to find a linear relation between γ-ray energy and channel number. This was accomplished by utilizing known γ-ray sources with different ranges of energies as presented in Table 1.

Table 1. The gamma ray energies of the three radioisotopes.

Sources	Energy 1 (keV)	Energy 2 (keV)	$T_{1/2}$ (y)
^{22}Na	511	1275	2.6
^{137}Cs	662	-	30.7
^{60}Co	1173	1333	5.7

The measurement process began with adjusting the power supply to 800 eV and placing the ^{137}Cs source in front of the scintillator with a fixed distance of 6.0 cm**.** The other sources were placed behind a lead shield to prevent the gamma radiation being emitting from them to be observed by the detector. The dynamic range of the ADC was optimized by locating the mean peak of ^{137}Cs gamma ray at approximately the middle of the range. Consequently, the photopeaks of higher gamma energies emitted from ^{60}Co and ^{22}Na can appear in the channel number scale. The acquisition time of the measurement was set at 3 minutes to obtain a reasonable statistic. As the photo peak in this spectrum follows the Gaussian shape distribution, fitting tools were used to locate the appropriate mean peaks that corresponds to specific channel number. Thus, certain parameters were extracted that describe the photopeak including FHWD, channel number, and the uncertainty in their values.

The calibration processes were repeated with the other sources to determine each gamma ray energy and its corresponding mean peak channel number. Thus, the root software is used to plot the graph of the linear relation between the obtained energies and channel numbers.

4-2 Resolution

The energy resolution of the NaI(TI) detector is obtained from the peak full width at one-half of the maximum height (FWHM) of a single peak using the following equation:

$$R = \frac{FWHM}{E_\gamma} = \frac{K}{\sqrt{E_\gamma}} \qquad (1)$$

where R is the energy resolution which is proportional of the related gamma energy E_γ and K is proportionality constant which characteristic of the particular detector. The FWHM is determined from the Gaussian Shape of each photo peaks as seen in Figure 2[10].

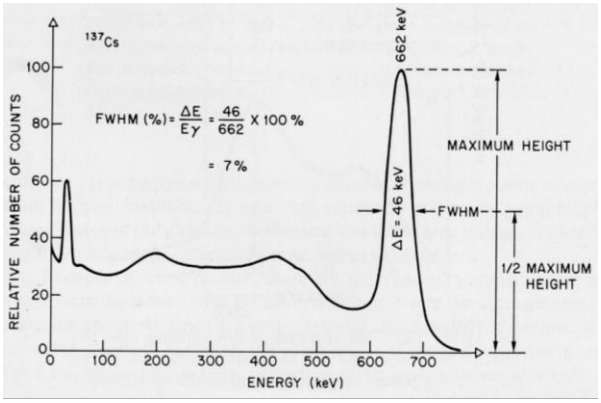

Figure 2. Calculation of the FWHM energy resolution of a NaI (Tl) detector for ^{137}Cs source (662 keV) [10].

4-3 Attenuation of Gamma Ray

The attenuation of the gamma ray was performed using the ^{137}Cs source, which produces 662 keV positioned at 6.0 cm distance from the detector face for a lead absorber (pb). This absorber (ρ_{Pb}=11.34 g/cm3) has different thicknesses as illustrated in Table 2, which are measured using a micrometer that has an error equal to ± 0.01.

Table 2. Shows a lead absorber having several thicknesses.

Thickness	**Pb(mm)**	**Error(mm)**
1	4.90	±0.01
2	9.81	±0.01
3	14.69	±0.01
4	19.53	±0.01

The energy spectra of the γ-rays emitted from ^{137}Cs source were plotted and fitted with the absence of any shield and with an absorbing material (Pb). This created

an individual attenuated and unattenuated γ-rays spectra obtained from ^{137}Cs source. As a result, the number of counts that is at the center of the acquired fitted prominent peaks was determined using root tools as represented in Figure 3.

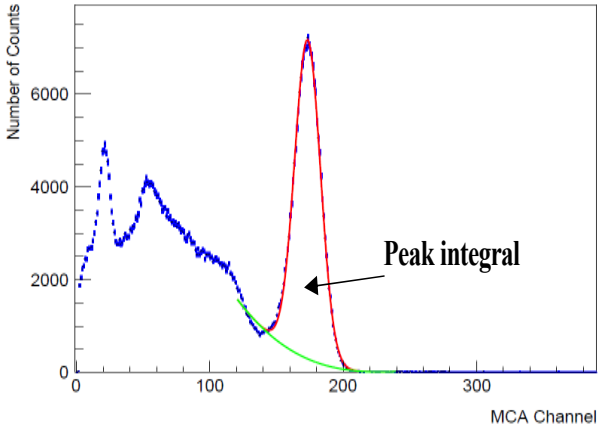

Figure 2. shows the peak integrals of calculation of the FWHM energy resolution of a NaI(Tl) detector for ^{137}Cs source(662 keV).

This step was applied for other spectrum to determine the intensity of γ-rays at each thickness. The statistical error of the intensity was calculated from the square root of the intensity σ =√intensity.

4.4 Absolute sensitivity Measurement

The number of counts emitted by the source differs from the number of detected counts by the detector. This is because not all the emitted pulses reach the detector (Geometric effect(ε_{geo})) and not all emitted pulses that reach the detector interact with its sensitive volume (detector intrinsic efficiency ($\varepsilon_{intrinsic}$). Therefore, the Absolute sensitivity can be determined as follow:

$$\text{Sensitivity}=\frac{Counts\ detected}{Counts\ calculated}=\frac{number\ of\ counts}{I_0 e^{-\lambda t}} \quad (2)$$

The counts detected $=I_0 e^{-\lambda t}\times \varepsilon_{geo}\times \varepsilon_{intrinsic}$

Thus,

$$\varepsilon_{intrinsic}=\frac{Sensitivity}{\varepsilon_{geo}}=\frac{Sensitivity}{\pi r^2/_{4\pi R^2}} \quad (3)$$

where r is the detector radius (r= 3.6 cm and 4.7 cm for the G-M detector and the b NaI(Tl) detector respectively) , and R is the distance between the detector and the radioactive source.

The activity of the ^{99}Tc source when it was prepared is I_0 = 190000Bq, therefore the strength of the source when the measurement started (I) after 4 hours (t = 4h) from its original activity (I_0) was:

$$\lambda=\frac{0.693}{t}=\frac{0.693}{6}=0.1155\ h^{-1} \quad (4)$$

Thus,

$$I=190000\ e^{-0.1155*4}=1197042\ Bq \quad (5)$$

5. Results and Discussion

5-1 Practical Use of Scintillation Counter (NaI (TI))

5-1-1 Calibration of The NaI (TI) scintillator

The energy calibration of the NaI (TI) scintillator has been achieved by plotting the pure spectrum of five γ-rays of the well-known sources shown in Table 1. Thus, each spectrum was fitted and the mean peak that corresponds to the incoming γ-rays energy was obtained as shown in Figures 3 and 4.

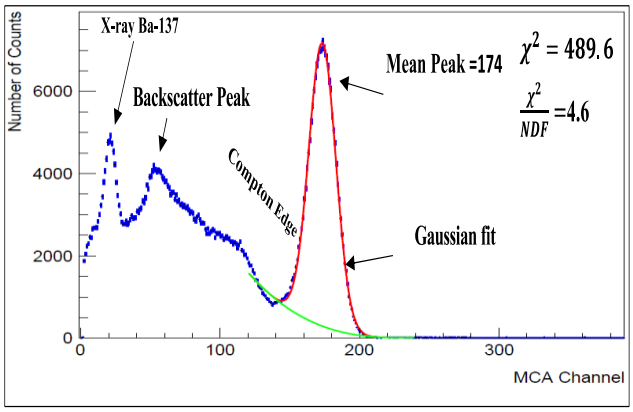

Figure 3. Shows the fitted Gaussian shape of the ^{137}Cs spectrum.

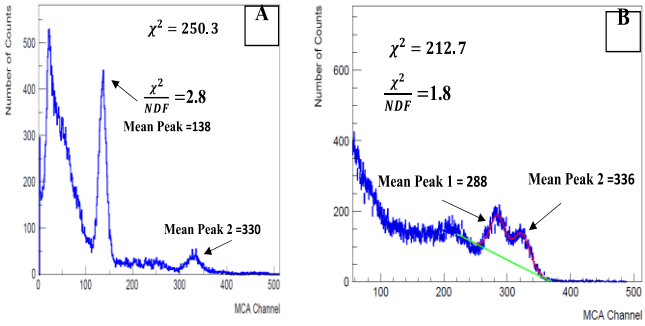

Figure 5. The fitted Gaussian shapes of 22Na (A) 60Co spectra (B).

The mean peaks that are at the center of the obtained fitted peaks and the systematic errors in their positions for all sources are shown in Table 3. The systematic errors were calculated by fitting each spectrum four times with various fitting scales and then determines the difference between the acquired mean peak positions.

Table 3. The mean peaks and their errors of the radioactive sources used to obtain calibration.

Sources	Energy (keV)	Mean Peak	Energy Error (keV)	Mean peak Error
^{22}Na	511.0	138.0	0.0	±1.0
^{137}Cs	662.0	174.0	0.0	±1.0
^{60}Co	1173.0	288.0	0.0	±1.0
^{22}Na	1275.0	330.0	0.0	±1.0
^{60}Co	1333.0	336.0	0.0	±1.0

The relation between the γ-ray energy and the channel numbers of the mean peaks of the given results was plotted using a straight-line fit. The integral of the peak positions is proportional to the incident γ-ray energy for all five energies, and thus the calibration values appeared on the same line as displayed in Figure 5.

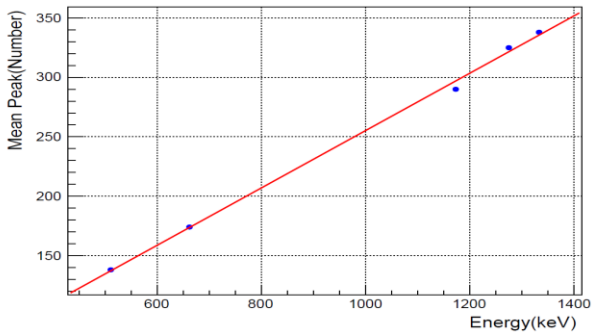

Figure 5. The energy calibration of the NaI(TI) scintillator as a function of a gamma ray energy with a linear fit.

As shown in Figure 5, the Y-intercept is 13.832 ± 1.387 (number) where the gradient is 0.241 ± 0.0013 number/keV. Therefore, this energy calibration can be utilize to determine the energy of any unknown gamma ray peak, which appears in the scintillator spectrum [11].

5-1-2 The FWHM and The Energy Resolution of NaI(TI)

The FWHM of each energy photo peak was calculated in order to determine energy resolutions of the NaI(Tl) detector which are presented in Table 4 and Figure 7.

Table 4. Energy resolution of the NaI(Tl) detector for several sources versus gamma ray energy.

Sources	Energy (keV)	FWHM	Resolution= F□□□% □□
^{22}Na	511.0	44.7	8.7
^{137}Cs	662.0	54.9	8.3
^{60}Co	1173.0	65.0	5.5
^{22}Na	1275.0	68.2	5.3
^{60}Co	1333.0	67.4	5.0

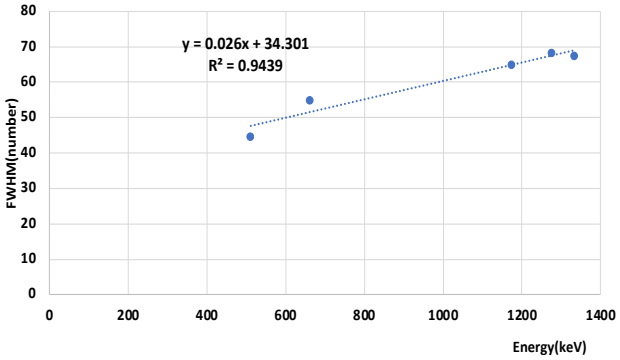

Figure 7. The FWHM of all of the five gamma rays as a function of the gamma ray energy.

As shown in Figure 7 the FWHM increases with the increase of the gamma ray energy. The resolution of the scintillator determines the ability to separate two overlapped or narrows peaks, which is directly proportional to gamma ray energies [8]. As presented in Table 4 the highest gamma rays have a better resolution, which reaches 5.06% and 5.53% for ^{60}Co.However, at lower energy such as ^{22}Na(511 keV), the resolution is relatively low (8.75%). This indicates that NaI(TI) is less efficient in identifying two adjacent energy peaks at low energy.

5-2 Absorption of gamma rays 5-2-1 calculating the linear attenuation coefficient of gamma ray

The intensities of the gamma ray emitted from ^{137}Cs (662 keV) after they penetrated different thicknesses of a lead shielding material were measured for all of the acquired fitted prominent peaks as shown in Tables 6.

Table 6. The variation of gamma-ray intensities as a function of shielding thickness (Pb) for ^{137}Cs source.

Thickness (mm)	Intensity (count)	Error in Thickness (mm)	Error in Intensity
0.0	166893	±0.0	± 408
5.04	104035	±0.1	± 322
10.06	57952	±0.1	± 240
15.09	33195	±0.1	± 182
21.14	18291	±0.1	± 135

Thus, the linear attenuation coefficient has been obtained by plotting an exponential function between the gamma ray intensities versus the various thicknesses of the absorber (Pb) as represented in Figure 8.

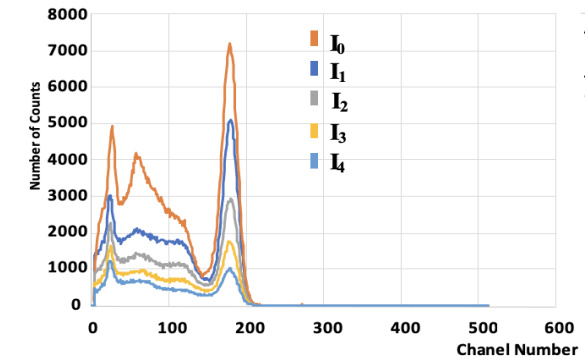

(a)

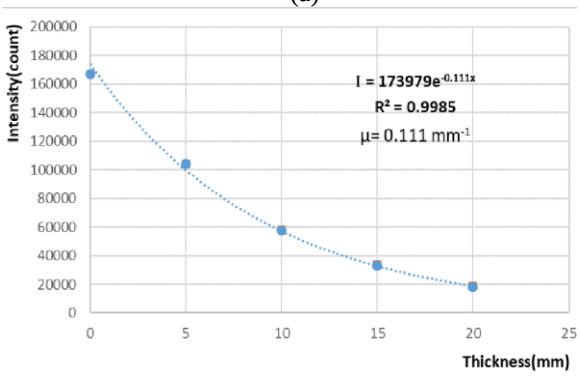

(b)

Figure 8. The attenuated gamma-ray intensities of ^{137}Cs as a function of shielding thickness of lead material, where I_0 represents the unattenuated gamma rays(a). The exponential reduction of gamma-ray intensities as a function of shielding thickness (Pb) for ^{137}Cs is displayed in (b).

The experiment results have revealed that the intensities of ^{137}Cs photo peaks were attenuated with an exponential decay due to the increase in thicknesses of the shielding material following the relationship mentioned in Eq.4. Therefore, the linear attenuation coefficient of the lead absorber (μ_{Pb}) obtained from the exponential fitting curves is 0.111 ± 0.006 mm^{-1} for ^{137}Cs source. This concludes that the lead absorber (ρ_{Pb}=11.34 g/cm^3) has a significant radiation attenuation property. Therefore, in medical application, The half-value thickness of lead is $X_{1/2}$ = 6.24 mm, which is calculated from Eq.5. Thus, higher thicknesses of lead shielding materials are essential to absorb gamma rays effectively [11].The practical results have been compared with the estimated value from the XCOM database as presented in Table 7. Thus, the results in Table 7 indicate that the attenuation coefficient of the lead absorber obtained from this experiment is in good agreement with the theoretical calculation. (12).

Table7. Comparison of the linear attenuation coefficient (μ_{Pb}) obtained with Xcom values. [13].

Source	μ_{Pb}-Experiment (mm^{-1})	μ_{Pb}-Xcom (mm^{-1})
^{137}Cs (662keV)	0.111	0.110

5-3 Absolute sensitivity Measurement

The absolute sensitivity and its corresponding error of both Geiger Muller detector and NaI(TI) scintillator was calculated at various distances as shown in Tables 8and 9 .The error in the distance is ± 0.1cm. The intrinsic efficiency and the geometric efficiency were calculated from Eq.8.

Table 8. Sensitivity of the G-M detector measured at various distances.

d(cm)	Number of Counts (cps)	Standard deviation of counts (√n)	sensitivity = $\frac{number\ of\ counts}{1.197}$ (cps/MBq)	Geometric Efficiency	Intrinsic Efficiency
5	50	±7.1	41.7 ± 5.9	0.0552	0.00075
10	17	±4.1	14.2 ± 3.4	0.0137	0.00122
15	12	±3.5	10.0 ± 2.9	0.0061	0.00191
20	5	±2.2	4.2 ± 1.8	0.0034	0.00122
30	2	±1.4	1.7 ± 1.2	0.0015	0.00111

Table 9. Sensitivity of the NaI(TI) detector measured at various distances.

d(cm)	Number of Counts (cps)	Standard deviation of counts (√n)	sensitivity = $\frac{number\ of\ counts}{1.197}$ (cps/MBq)	Geometric Efficiency	Intrinsic Efficiency
10	3500	±59.1	2923.9 ± 49.3	0.0081	0.360972
15	1800	±42.4	1503.7 ± 35.4	0.0036	0.464107
20	1200	±34.6	1002.5 ± 28.9	0.0020	0.501235
30	500	±22.4	417.7 ± 18.7	0.0009	0.464107

As shown in Table 8 the sensitivity of the Geiger Muller counter and NaI(TI) detector decreased significantly with the increase of distance from the 99Tc source(a proportional inverse). The sensitivity for G-M and NaI(TI) detector and at 10 cm ± 0.1cm from the source were 14.2 cps/MBq ± 3.4 cps/MBq and 2923.9 cps/MBq ± 49.3 /MBq respectively. While at a distance of 30 cm ± 0.1cm, the sensitivity was only 1.7 cps/MBq ± 1.2 cps/MBq for the G-M detector compared with 417.7 cps/MBq ± 18.7 cps/MBq measured by NaI(TI) detector. This indicates that the G-M counter is considerably low sensitive to gamma radiaition, wherese the NaI(TI) scintialtor has a high sensitivity for detection and estimation of radionuclides such as 99Tc. Consequently, for a medical use, NaI(TI) detector has a better detection sensitivity for the gamma ray emitted from the patient organ.

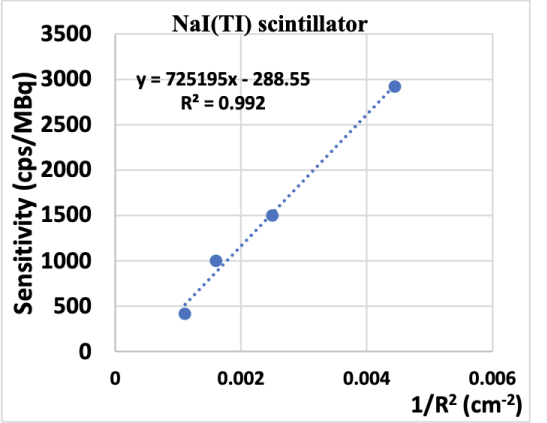

(a)

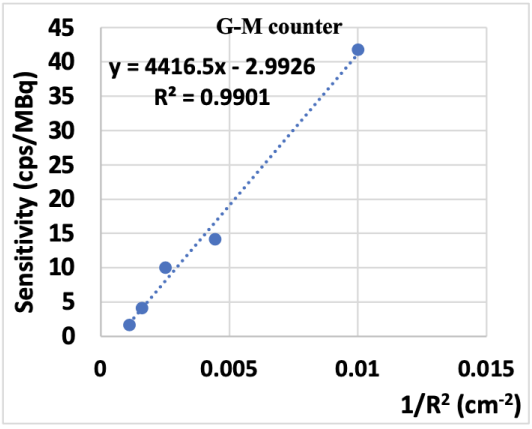

(b)

Figure 9. The linear relationship between the inverse square and the sensitivity of the Geiger Muller detector (a) and the NaI(TI) scintillator (b).

The inverse square law was verified as displayed in Figure 9, where the sensitivity of both G-M detector and NaI(TI) scintillator is directly proportional to the inverse squared distance from the 99Tc source.

6- Conclusion

The determination of attenuation properties of electromagnetic radiation in any absorbing materials are of great importance for radiation shielding purposes in applied nuclear radiation fields. The attenuation efficiencies and shielding effectiveness of lead was experimentally investigated by using the NaI(TI) scintillator. The results revealed that lead is an effective shielding material for gamma ray with a high linear attenuation coefficient (μ!" = 0.111□□()) .Moreover, the practical result of the linear attenuation coefficient in this study is in satisfactory agreement with the XCOM calculation. Furthermore, the sensitivity of both the G-M counter and the NaI(TI) scintillator was determined as a function of distance from a99Tc source. The experimental findings showed that the NaI(TI) detector is significantly sensitive to gamma ray radiation compared with a very low sensitivity was obtained by the G-M counter. Consequently, this present experiment concludes that the NaI(TI) is a suitable detector for detection purposes in medical applications. Therefore, for radiation measurement and protection, future work can be built on this experiment to determine the linear attenuation coefficients for various absorbing materials at different energies, as well as the sensitivity of other type of detectors.

References

[1] Al-Sarray E, Akkurt İ, Günoğlu K, Evcin A, Bezir NÇ. Radiation Shielding Properties of Some Composite Panel. Acta Physica Polonica, A.. 2017 Sep 1;132(3).

[2] Akkurt I, Gunoglu K, Arda SS. Detection Efficiency of NaI (Tl) Detector in 511–1332 keV Energy Range.

[3] Elbashir BO, Dong MG, Sayyed MI, Issa SA, Matori KA, Zaid MH. Comparison of Monte Carlo simulation of gamma ray attenuation coefficients of amino acids with XCOM program and experimental data. Results in Physics. 2018 Jun 1;9:6-11.

[4] Allisy-Roberts P, Williams JR. Farr's physics for medical imaging. Elsevier Health Sciences; 2007.

[5] Oliván MA, Amaré J, Cebrián S, Cuesta C, García E, Martínez M, Ortigoza Y, de Solórzano AO, Pobes C, Puimedón J, Sarsa ML. Light yield determination in large sodium iodide detectors applied in the search for dark matter. Astroparticle Physics. 2017 Jul 1;93:86-95.

[6] ELIJAH, K., 2016. *RADIOACTIVITY CONCENTRATIONS AND DOSE ASSESSMENT FOR SOIL SAMPLES FROM WHEAT PLANTATION AREAS OF NAROK COUNTY, KENYA*(Doctoral dissertation, Kenyatta University).

[7] Pandey S, Pandey A, Deshmukh M, Shrivastava AK. Role of Geiger Muller Counter in Modern Physics. Journal of Pure Applied and Industrial Physics. 2017 May;7(5):192-6.

[8] Cherry SR, Sorenson JA, Phelps ME. Physics in nuclear medicine e-Book. Elsevier Health Sciences; 2012 Feb 14.

[9] Ahmadi S, Ashrafi S, Yazdansetad F. A method to calculate the gamma ray detection efficiency of a cylindrical NaI (Tl) crystal. Journal of Instrumentation. 2018 May 14;13(05):P05019.

[10] Tarim UA, Gurler O. Source-to-detector Distance Dependence of Efficiency and Energy Resolution of a 3" x3" NaI (Tl) Detector. Avrupa Bilim ve Teknoloji Dergisi. 2018 Aug 31(13):103-7.

[11] Sukara S, Rimjeam S. Simulation of Gamma Rays Attenuation Through Matters Using the Monte Carlo Program. InJournal of Physics: Conference Series 2017 Sep (Vol. 901, No. 1, p. 012141). IOP Publishing.

[12] Zhang L, Jia M, Gong J, Xia W. Comparison study of photon attenuation characteristics of Lead-Boron Polyethylene by MCNP code, XCOM and experimental data. Radiation Effects and Defects in Solids. 2017 Aug 3;172(7-8):643-9.

[13] *NIST X-ray photoelectron spectroscopy database*. Measurement Services Division of the National Institute of Standards and Technology (NIST) Technology Services, 2008.

2/16/2024